Influence of microstructural features on the effective magnetostriction of composite materials

Ce-Wen Nan
Advanced Materials Research Institute, Wuhan University of Technology, Wuhan, Hubei 430070, China
and Department of Mechanical & Aerospace Engineering, Rutgers University, New Brunswick, New Jersey 08903

G. J. Weng
Department of Mechanical & Aerospace Engineering, Rutgers University, New Brunswick, New Jersey 08903
(Received 16 March 1999)

Recently developed magnetostrictive composites of a giant magnetostrictive alloy and an inactive matrix have opened up a promising territory for the application of materials with magnetic-mechanical coupling interactions. In this article an effective-medium method is developed for the effective magnetostrictive behavior of such composite materials based on a Green's-function technique. Explicit relations for determining the effective magnetostriction of the spherical particulate and fibrous composites with elastically isotropic magnetostrictive crystallites are derived. Two extreme bounds—the Reuss and Voigt-type bounds—are also given. To illustrate the technique, numerical calculations for the effective saturation magnetostriction of $SmFe_2$/epoxy or aluminum and Terfenol-D/epoxy or aluminum composites with various phase compositions, particle shapes and orientation, and crystallite growth directions, are performed. The theoretical estimates are found to be in agreement with available experimental results, and they also show the interesting magnetostrictive behavior of the composites. [S0163-1829(99)01933-5]

I. INTRODUCTION

Magnetostrictive materials whereby magnetization produces deformation and, conversely, deformation affects magnetization, have received much attention in recent years. Of particular interest because of its comparatively large magnetostriction is the rare-earth-iron alloys such as Terfenol-D, the magnetostriction of which under the influence of even a small field can be as much as 10^{-3}.[1] These materials can be used in sensors and actuators in state-of-the-art technology, such as ultrasound devices, automobiles, and aircrafts. However, these materials having giant magnetostriction are both expensive and brittle. On the other hand, stronger and tougher magnetostrictive metals (e.g., Ni) have very small magnetostriction ($\sim$30 ppm).[1,2] An effective way to combine large magnetostriction with good mechanical properties is the fabrication of machinable magnetostrictive composites. Recently there have been an increasing interest in development of these magnetostrictive composites.[3–8] By combining a giant magnetostrictive material with a compliant inactive polymer[3,4,7] or a metal,[5,6,8] the composite magnetostrictive actuators can be mechanically flexible with intermediate magnetostriction. Although there is an increasing emphasis on the practical development of such a composite, fundamental understanding of its effective magnetostrictive behavior is rather limited and little published data is available describing its magnetostrictive response, which is essential to any technical improvements of such magnetostrictive composites.

The magnetostrictive effect is a nonlinearly coupled mechanical-magnetic phenomenon, and is a very complicated problem, especially for inhomogeneous magnetostrictive materials due to complicated microstructure. By analogy to the elastic problem of polycrystals, the first Reuss and Voigt-type approximations for the saturation magnetostriction of a simple isotropic polycrystal consisting of cubic microcrystals were derived.[2,9–11] The most commonly used formula for estimating the effective saturation magnetostriction $\overline{\lambda_s}$ of such an isotropic polycrystal is a Reuss-type approximation by which $\overline{\lambda_s}$ is obtained as a linear function of the single-crystal magnetostriction constants $(\lambda_{100}, \lambda_{111})$,[1,2] i.e.,

$$\overline{\lambda_s} = a\lambda_{100} + (1-a)\lambda_{111} \tag{1}$$

with $a = 2/5$ for elastically isotropic microcrystals.[1,2]

For magnetostrictive composites recently developed, Herbst, Capehart, and Pinkerton[6] have proposed a simple single-sphere model, i.e., an idealized single-particle problem for elastically isotropic magnetostrictive composites, in which an elastically isotropic magnetostrictive particle is embedded in an isotropic nonmagnetostrictive matrix. They have derived an almost *universal* expression for the effective magnetostriction of such magnetostrictive composites, which is nearly insensitive to material elastic constants of the constituents. However, in the limit of only a single magnetostrictive phase (i.e., single-phase magnetostrictive polycrystal), this expression yields an incorrect prediction, for the interaction among magnetostrictive particles are totally ignored in this single-sphere model.

In this paper, we present a detailed theoretical study of the effective magnetostrictive behavior of magnetostrictive composites. The principal motivation has been to investigate what role the complicated microstructure of an inhomogeneous magnetostrictive material plays in its magnetostrictive behavior. The present work is a sequel to an earlier brief publication,[12] in which a formula for the effective magnetostriction of an elastically isotropic magnetostrictive composite has been given based on a Green's-function technique.[13] Here we are concerned with more general cases, and consider the sensitivity of the magnetostrictive effect for mag-

netostrictive composites on the material constants and microstructure, such as anisotropy, particle shape, and orientation relative to the applied magnetic field.

The essence of the present problem is to calculate the strong magnetoelastic coupling interaction of an inhomogeneous medium. The low-signal, linearly coupled magnetoelastic (i.e., piezomagnetic) properties of inhomogeneous media was successfully treated previously by Nan[14] using a Green's-function technique (a multiple-scattering method in the sense of Zeller-Dederichs and Gubernatis-Krumhansl[13]) developed for the linearly electroelastic coupling problem.[15] This technique is also valid for nonlinear problems with large fluctuations, although its exact realm of validity is very hard to ascertain. In the present work, we shall extend this approach to address the nonlinearly coupled magnetic-mechanical behavior, e.g., magnetostriction of magnetostrictive composites.

Section II contains the theoretical framework derived by the multiple-scattering method and the general solution to the effective magnetostriction of the inhomogeneous magnetostrictive materials. In Sec. III, without loss of generality, we mainly consider magnetostrictive microcrystallites with cubic symmetry embedded in a matrix, and give explicit expressions for the effective saturation magnetostriction of two technologically important composites: spherical particulate and fibrous composites with elastically isotropic crystallites. For illustrative and quantitative purposes, the numerical results for the effective saturation magnetostriction of composites in the important systems of $SmFe_2$/epoxy or Al and Terfenol-D/epoxy or Al are presented for various microstructural features in Sec. IV. In our calculations, $SmFe_2$ is considered as elastically isotropic, while Terfenol-D is considered as cubic for illustration. The conclusions are summarized in Sec. V.

II. GENERAL FRAMEWORK

The magnetic-mechanical coupling behavior of a material with magnetomechanical interactions can be described by the following constitutive equations:

$$\sigma = \mathbf{C}\varepsilon - \mathbf{q}^{\mathbf{T}}\mathbf{H} - \chi^{\mathbf{T}}\mathbf{H}\mathbf{H} - \beta\Delta T, \tag{2}$$

$$\mathbf{B} = \mathbf{q}\varepsilon + \mu\mathbf{H} + \chi\varepsilon\mathbf{H} + \mathbf{p}\Delta T, \tag{3}$$

where σ, ε, $\mathbf{B}$, and $\mathbf{H}$, are the stress tensor, strain tensor, magnetic induction (or flux density), and magnetic field, respectively; T is temperature; $\mathbf{q}$ ($\mathbf{q}^T$ being the transpose of $\mathbf{q}$) is the piezomagnetic coefficient in the low signal linear region; χ is magnetostrictive coefficient (χ^T being the transpose of χ); $\mathbf{C}$ and μ are, respectively, the stiffness and permeability tensors; $\mathbf{p}$ is the pyromagnetic coefficient, $\beta = \mathbf{C}\alpha$ and α is the thermal-expansion coefficient. For simplicity, we have used the direct notation for tensors.

The constitutive equations above contain two magnetomechanical effects: piezomagnetic and magnetostrictive effect. The piezomagnetic effect is a linear magnetic-elastic interaction, i.e., generation of magnetization by mechanical means in the *absence* of a magnetic field or conversely a material becoming strained when subjected to a magnetic field. This linear piezomagnetic effect is completely analogous to the linear piezoelectric effect, which has been treated in detail.[14–16] The magnetostrictive effect is a nonlinear magnetomechanical interaction, i.e., magnetostriction which is a geometric distortion of a material that occurs in response to an applied magnetic field. There exists also an inverse magnetostrictive effect which causes magnetization to be strongly dependent on stress in the *presence* of a magnetic field. This inverse magnetostrictive effect is different from the direct piezomagnetic effect. In a demagnetized material, a stress will not produce any magnetization. In comparison with the piezomagnetism, which is a seldom encountered linearly coupling effect because of the stringent symmetry properties required for its existence, the nonlinearly coupling magnetostriction is an ever existing effect in all materials to be studied for practical applications. In the cubic magnetostrictive crystals with the giant magnetostrictive effect considered here, there does not exist piezomagnetic effect. After ignoring the piezomagnetic effect, Eqs. (2) and (3) can simply be rewritten as

$$\sigma = \mathbf{C}(\varepsilon - \varepsilon^{\mathrm{ms}}) - \beta\Delta T, \tag{4}$$

$$\mathbf{B} = \mu\mathbf{H} + \mathbf{p}\Delta T, \tag{5}$$

where the permeability μ strongly depends on ε and $\mathbf{H}$, and $\varepsilon^{\mathrm{ms}}$ is the magnetostrictively induced strain.

The effective magnetostrictive behavior of an inhomogeneous material is defined in terms of averaged fields (denoted by $\langle\ \rangle$), namely

$$\langle\sigma\rangle = \mathbf{C}^*(\langle\varepsilon\rangle - \overline{\varepsilon}^{\mathrm{ms}}) - \beta^*\Delta T, \tag{6}$$

$$\langle\mathbf{B}\rangle = \mu^*\langle\mathbf{H}\rangle + \mathbf{p}^*\Delta T. \tag{7}$$

Therefore, the problem of evaluating the effective response of the material essentially consists of the determination of the field variables within it under certain specified boundary conditions, followed by the performance of the averages.

The simplest methods for solving the problem are the Reuss and Voigt-type average approximations which can directly be given from these equations. For brevity, we consider the pure magnetostrictive case of $\langle\sigma\rangle = 0$ (i.e., no external stress) and by neglecting the thermal effect. By assuming that the stress is the same in all crystallites (phases), i.e., $\sigma^{(i)} = \langle\sigma\rangle = 0$, which means each crystallite may expand freely, one obtains the Reuss-type approximation of the effective magnetostrictive strain simply by taking the average value of the strains induced in all the crystallites, namely,

$$\overline{\varepsilon}^{\mathrm{ms}} = \langle\varepsilon\rangle = \langle\varepsilon^{\mathrm{ms}}\rangle, \tag{8}$$

which further reduces to the commonly used Eq. (1) for the isotropic polycrystal consisting of elastically isotropic microcrystals (see Sec. III A). Similarly, to the other extreme, by assuming that the strain is the same in all crystallites (phases), i.e., $\varepsilon^{(i)} = \langle\varepsilon\rangle (= \overline{\varepsilon})$, one obtains the Voigt-type approximation of the effective magnetostrictive strain

$$\overline{\varepsilon}^{\mathrm{ms}} = \langle\mathbf{C}\rangle^{-1}\langle\mathbf{C}\varepsilon^{\mathrm{ms}}\rangle = (\overline{\mathbf{C}})^{-1}\langle\mathbf{C}\varepsilon^{\mathrm{ms}}\rangle. \tag{9}$$

For a single-phase polycrystal, the average values are taken over all possible orientations and Eq. (9) is exactly the expression given recently by Birsan.[11] The Reuss and Voigt-type approximations yield a sort of rough bound of the ef-

fective magnetostriction. Next we develop an effective-medium approach for the effective magnetostriction.

Because of spatial variation in the constitutive behavior in the material with position, the local constitutive coefficients can be written as a variation about a mean value

$$\mathbf{C}(\mathbf{x})=\mathbf{C}^o+\mathbf{C}'(\mathbf{x}),\mu(\mathbf{x})=\mu^o+\mu'(\mathbf{x}),$$

$$\beta(\mathbf{x})=\beta^o+\beta'(\mathbf{x}),\mathbf{p}(\mathbf{x})=\mathbf{p}^o+\mathbf{p}'(\mathbf{x}), \tag{10}$$

where the first terms (denoted by superscripts o) represent the constitutive constants of a homogeneous reference medium and the second terms are the spatial fluctuation with respect to the first.

To proceed, let the material be now subjected on its external surface S to a homogeneous magnetic-mechanical boundary condition, i.e.,

$$u_i(S)=\varepsilon^o_{ij}x_j=u^o_i,\phi(S)=-H^o_i x_i=\phi^o, \tag{11}$$

where u_i and ϕ denote elastic displacement and magnetic potential, respectively. In a state of static equilibrium,

$$\sigma_{ij,j}(\mathbf{x})=0,B_{j,j}(\mathbf{x})=0, \tag{12}$$

where the commas in the subscripts denote partial differentiation with respect to x_j.

Further by solving the equilibrium equations under the boundary conditions (11) by means of the Green's-function technique, the local strain and magnetic field within the material can be obtained as

$$\varepsilon=\varepsilon^o+\mathbf{G}^u\mathbf{C}'\varepsilon-\mathbf{G}^u\mathbf{C}\varepsilon^{\mathrm{ms}}-\mathbf{G}^u\beta\Delta T, \tag{13}$$

$$\mathbf{H}=\mathbf{H}^o+\mathbf{G}^\phi\mu'\mathbf{H}+\mathbf{G}^\phi\mathbf{p}\Delta T, \tag{14}$$

where ε^o and $\mathbf{H}^o$ are the strain and magnetic field in the homogeneous reference medium at equilibrium, and $\mathbf{G}^u$ and $\mathbf{G}^\phi$ are the modified displacement and magnetic potential Green's functions for the homogeneous medium.[15] Iterative solutions of Eqs. (13) and (14) yield

$$\varepsilon=\mathbf{T}^{66}\varepsilon^o-\mathbf{T}^{66}\mathbf{G}^u\mathbf{C}\varepsilon^{\mathrm{ms}}-\mathbf{T}^{66}\mathbf{G}^u\beta\Delta T, \tag{15}$$

$$\mathbf{H}=\mathbf{T}^{33}\mathbf{H}^o+\mathbf{T}^{33}\mathbf{G}^\phi\mathbf{p}\Delta T, \tag{16}$$

with

$$\mathbf{T}^{66}=(\mathbf{I}-\mathbf{G}^u\mathbf{C}')^{-1},$$

$$\mathbf{T}^{33}=(\mathbf{I}-\mathbf{G}^\phi\mu')^{-1},$$

where $\mathbf{I}$ is the unit tensor.

By averaging these equations and eliminating ε^o and $\mathbf{H}^o$ from them, we get the general solutions to the effective behavior of the material

$$\mathbf{C}^*=\langle\mathbf{C}\mathbf{T}^{66}\rangle\langle\mathbf{T}^{66}\rangle^{-1}, \tag{17}$$

$$\mu^*=\langle\mu\mathbf{T}^{33}\rangle\langle\mathbf{T}^{33}\rangle^{-1}, \tag{18}$$

$$\overline{\varepsilon}^{\mathrm{ms}}=(\mathbf{C}^*)^{-1}\langle[(\mathbf{C}-\mathbf{C}^*)\mathbf{T}^{66}\mathbf{G}^u+\mathbf{I}]\mathbf{C}\varepsilon^{\mathrm{ms}}\rangle, \tag{19}$$

$$\alpha^*=(\mathbf{C}^*)^{-1}\langle[(\mathbf{C}-\mathbf{C}^*)\mathbf{T}^{66}\mathbf{G}^u+\mathbf{I}]\mathbf{C}\alpha\rangle, \tag{20}$$

$$\mathbf{p}^*=\langle[(\mu-\mu^*)\mathbf{T}^{33}\mathbf{G}^\phi+\mathbf{I}]\mathbf{p}\rangle. \tag{21}$$

Equations (17), (18), and (20) are the commonly used effective-medium expressions for the effective stiffness, permeability, and thermal-expansion coefficient. The effective magnetostrictive strain tensor exhibits the same apparent expression as the effective thermal-expansion coefficient tensor. Now the macroscopic strain of the material is obtained as

$$\langle\varepsilon\rangle=(\mathbf{C}^*)^{-1}\{\langle\sigma\rangle+\langle[(\mathbf{C}-\mathbf{C}^*)\mathbf{T}^{66}\mathbf{G}^u+\mathbf{I}]\mathbf{C}(\varepsilon^{\mathrm{ms}}+\alpha\Delta T)\rangle\}. \tag{22}$$

The total strain consists of three contributions: the effective deformation due to external stress, i.e., $(\mathbf{C}^*)^{-1}\langle\sigma\rangle$, the effective magnetostrictively induced deformation, and thermal strain. These results are general and independent of the models assumed for the material and contain the effects of materials constants, microstructural features, applied fields, and temperature. Given the properties of magnetostrictive microcrystallites, the macroscopic behavior (such as magnetostriction, hysteresis, stress, and thermal effect, and ΔE effect—change in Young's modulus E with magnetic bias[1,2]) of the inhomogeneous magnetostrictive materials can be well quantitatively assessed by using the above methodology. Without limiting the generalization of the approach, we next focus upon only the effective magnetostriction.

III. EFFECTIVE MAGNETOSTRICTION OF COMPOSITES CONTAINING CRYSTALLITES WITH CUBIC SYMMETRY

Let us consider an inhomogeneous material containing magnetostrictive microcrystallites with cubic symmetry that most commonly reported giant magnetostrictive crystals exhibit.[1] In this case, the local magnetostrictive strains along the crystallographic axes of a microcrystallite can be obtained as[17]

$$\varepsilon^{\mathrm{ms}}_{ij}=\begin{cases}\lambda^\alpha+\frac{3}{2}\lambda_{100}\left(\alpha^2_{3i}-\frac{1}{3}\right), & \text{for } i=j,\\ \frac{3}{2}\alpha_{3i}\alpha_{3j}\lambda_{111}, & \text{for } i\neq j\end{cases}, \tag{23}$$

where λ_{100}, λ_{111}, and λ^α are the usual magnetostriction constants of the cubic microcrystallite, (α_{ij}) is the matrix transforming the local crystallographic axes X'_j to the materials axes X_i, in which an external magnetic field $\overline{H}_3$ is applied along the X_3 axis of the materials sample, namely, $X_i=\alpha_{ij}X'_j$, and

$$(\alpha_{ij})=\begin{pmatrix}\cos\phi\cos\psi-\sin\phi\sin\psi\cos\theta & -\cos\phi\sin\psi-\sin\phi\cos\psi\cos\theta & \sin\phi\sin\theta\\ \sin\phi\cos\psi+\cos\phi\sin\psi\cos\theta & -\sin\phi\sin\psi+\cos\phi\cos\psi\cos\theta & -\cos\phi\sin\theta\\ \sin\psi\sin\theta & \cos\psi\sin\theta & \cos\theta\end{pmatrix}, \tag{24}$$

where θ is the angle between X_3 and X_3', and ψ and ϕ are, respectively, the usual Euler angles in the $X_1'X_2'$ plane and X_1X_2 plane (perpendicular $\overline{H}_3$). Substituting Eq. (23) into Eq. (19) determines the effective magnetostriction of the materials. For illustrative purposes, we consider such inhomogeneous materials with two crystallite geometries: (a) spherical magnetostrictive crystallites and (b) cylindrical crystallites (fibers) with various growth directions.

A. Spherical magnetostrictive crystallites

Let us first consider a two-phase particulate composite consisting of a volume fraction f of spherical magnetostrictive crystallites and a nonmagnetostrictive (with negligible magnetostrictive effect), isotropic phase. The most simple case is that all the spherical magnetostrictive crystallites are ideally elastically isotropic, i.e., $c_{11}-c_{12}=2c_{44}$ (c_{ij} being the elastic constants of the spherical magnetostrictive crystallites). In this case, we can easily obtain the macroscopically magnetostrictive strains parallel and perpendicular to the applied magnetic field $\overline{H}_3$, $\overline{\varepsilon}_{\parallel}^{\rm ms}$, and $\overline{\varepsilon}_{\perp}^{\rm ms}$, from the effective-medium formulas above as

$$\overline{\varepsilon}_{\parallel}^{\rm ms}=f\lambda^{\alpha}(E_{11}+2E_{12})+2f\lambda_{100}E_{44}+3fE_{44}(\lambda_{111}-\lambda_{100})\left(1-\left\langle\sum_{i=1}^{3}\alpha_{3i}^4\right\rangle\right), \tag{25}$$

$$\overline{\varepsilon}_{\perp}^{\rm ms}=f\lambda^{\alpha}(E_{11}+2E_{12})-f\lambda_{100}E_{44}-3fE_{44}(\lambda_{111}-\lambda_{100})\times\left\langle\sum_{i=1}^{3}\alpha_{1i}^2\alpha_{3i}^2\right\rangle, \tag{26}$$

where the first term, $f\lambda^{\alpha}(E_{11}+2E_{12})$, in both $\overline{\varepsilon}_{\parallel}^{\rm ms}$ and $\overline{\varepsilon}_{\perp}^{\rm ms}$ is the volume magnetostriction effect, and E_{ij} are the components of the following tensor:

$$\mathbf{E}=[\mathbf{I}-\mathbf{G}^u(\mathbf{C}^*-\mathbf{C}^o)][\mathbf{I}-\mathbf{G}^u(\mathbf{C}-\mathbf{C}^o)]^{-1}(\mathbf{C}^*)^{-1}\mathbf{C}. \tag{27}$$

Therefore, the effective engineering magnetostriction $\overline{\lambda}_s$ of the elastically isotropic composite is obtained as[12]

$$\overline{\lambda}_s=\frac{2}{3}(\overline{\varepsilon}_{\parallel}^{\rm ms}-\overline{\varepsilon}_{\perp}^{\rm ms}) \tag{28}$$

$$=\frac{1-G_1/G^*}{1-G_1/G_2}\left[\lambda_{111}+(\lambda_{111}-\lambda_{100})\times\left\langle\sum_{i=1}^{3}(\alpha_{1i}^2\alpha_{3i}^2-\alpha_{3i}^4)\right\rangle\right], \tag{29}$$

where G_1, G_2, and G^* are the shear moduli of the nonmagnetostrictive matrix, magnetostrictive crystallites, and the composite, respectively. Equation (29) clearly demonstrates that the effective magnetostriction of such isotropic composites depends on the volume fraction and all related material constants as well as the orientation of the crystallites in the composites.

Accordingly, Eqs. (8) and (9) yield the Reuss and Voigt-type bounds in such an elastically isotropic case, namely,

$$\overline{\lambda}_s^{\rm Reuss}=f\left\{\lambda_{111}+(\lambda_{111}-\lambda_{100})\left\langle\sum_{i=1}^{3}(\alpha_{1i}^2\alpha_{3i}^2-\alpha_{3i}^4)\right\rangle\right\}, \tag{30}$$

$$\overline{\lambda}_s^{\rm Voigt}=f\frac{G_2}{\overline{G}}\left\{\lambda_{111}+(\lambda_{111}-\lambda_{100})\left\langle\sum_{i=1}^{3}(\alpha_{1i}^2\alpha_{3i}^2-\alpha_{3i}^4)\right\rangle\right\}, \tag{31}$$

with $\overline{G}=(1-f)G_1+fG_2$. Obviously, the Voigt-type relation yields an upper bound as $G_1<G_2$, and a lower bound as $G_1>G_2$.

As $f=0$ (i.e., a single-phase nonmagnetostrictive materials), $G^*=G_1$ and so $\overline{\lambda}_s=0$. As $f=1$, i.e., for a single-phase, elastically isotropic polycrystal, $G^*=G_2$, so the effective-medium formulas, and the Reuss and Voigt-type bounds superpose together, and thus yield an exact result for such an idealized polycrystal, namely,

$$\overline{\lambda}_p=\lambda_{100}+(\lambda_{111}-\lambda_{100})\left[1-\left\langle\sum_{i=1}^{3}(\alpha_{3i}^4-\alpha_{1i}^2\alpha_{3i}^2)\right\rangle\right]. \tag{32}$$

It is easy to show that $\overline{\lambda}_p=(2\lambda_{100}+3\lambda_{111})/5$, i.e., Eq. (1) for the random orientation and $\overline{\lambda}_p=\lambda_{111}$ for the perfectly preferred orientation (i.e., the $\langle 111\rangle$ directions of all magnetostrictive crystallites being identically parallel to the applied magnetic field $\overline{H}_3$). These are two well-known simple but exact results for the elastically isotropic polycrystals of elastically isotropic crystallites with $c_{11}-c_{12}=2c_{44}$.[1,2]

B. Aligned magnetostrictive rods

We now consider a special but technologically important composite having the so-called 1-3 connectivity of phases (in the terminology introduced by Newnham, Skinner, and Cross[18]), in which cylindrical magnetostrictive rods embedded in a nonmagnetostrictive matrix are aligned parallel applied magnetic field $\overline{H}_3$ (the sample axis X_3). For elastically isotropic magnetostrictive rods with the aspect ratio (=length/diameter)$\rightarrow\infty$, similarly, we find its effective engineering magnetostriction $\overline{\lambda}_s$ from expression (19) as

$$\overline{\lambda}_s=\frac{fm_2}{c_{33}^*k^*-(c_{13}^*)^2}\{2F(2k^*+c_{13}^*)+(c_{33}^*+2c_{13}^*)(k^*+m_1)/(k_2+m_1)\}\overline{\lambda}_{\theta}, \tag{33}$$

TABLE I. Properties of $SmFe_2$ and Terfenol-D magnetostrictive crystallites, and epoxy and metal matrix to be taken in the present numerical calculations.

	$SmFe_2$	Terfenol-D	Epoxy	Al
c_{11}(GPa)	82	101	6.5	101
c_{12}(GPa)	66	40	3.5	49
c_{44}(GPa)	22	38	1.5	26
λ_{111}(ppm)	−2100	1700		
λ_{100}(ppm)	−700	100		

with

$$F=1-\frac{(c_{13}^*-k^*)(k_2+m_1)+k_1(k^*-k_2)+m_2(k^*+m_1)}{(k_2+m_1)(k_1+m_1)},$$

where $2k^*=c_{11}^*+c_{12}^*$ (i.e., the transverse bulk modulus) and $2m^*=c_{11}^*-c_{12}^*$ (i.e., the transverse shear modulus), and the same relations hold for k_2 (k_1) and m_2 (m_1). For comparison, here we still use Eq. (28) to define its effective saturation magnetostriction.

$\bar{\lambda}_\theta$ in Eq. (33) is dependent on the direction along which the magnetostrictive fibers preferentially grow. For the fibers with their preferred growth direction along $\langle 112\rangle$, for instance,

$$\bar{\lambda}_\theta=(\lambda_{100}+3\lambda_{111})/12. \tag{34}$$

For the perfectly preferred $\langle 111\rangle$ growth direction,

$$\bar{\lambda}_\theta=\lambda_{111}/3. \tag{35}$$

Again, of interest to note is that as $f=1$, i.e., for a single-phase polycrystal of such elastically isotropic magnetostrictive crystallites, $\bar{\lambda}_s=3\bar{\lambda}_\theta$. This result is the same as that given by Eq. (32) for such a special case.

IV. NUMERICAL RESULTS AND DISCUSSIONS

In order to have better understanding of the theoretical results above, we perform numerical computation for the magnetostrictive composites. For quantitative purpose, $SmFe_2$/epoxy or Al, and Terfenol-D/epoxy or Al composites are considered. The properties of the constituent phases used for calculations are given in Table I. Here $SmFe_2$ is considered to be elastically isotropic for illustration. A comparison between the calculations and reported experimental data for the magnetostriction of elastically isotropic $SmFe_2$/Al and $SmFe_2$/Fe composites[6] has demonstrated that our calculations are in agreement with the experimental data.[12] Next we mainly evaluate the influences of material constants and microstructural features on the effective saturation magnetostriction of the composites.

A. Spherical particulate composites

Figure 1 shows the effective saturation magnetostriction $\bar{\lambda}_s$ for randomly oriented spherical $SmFe_2$ particles, reinforced Al or epoxy matrix composites. It clearly demonstrates that the elastic constants of the inactive matrix have a pronounced effect on the effective magnetostriction. For Al-matrix composites, the effective magnetostriction almost linearly increases with the volume fraction f due to the closer elastic moduli of the Al matrix and the magnetostrictive particles, while the effective magnetostriction for epoxy matrix composites are larger than that for the Al composites. This indicates that the effective magnetostriction of the composites can increase through the use of mechanically softer matrices, which is directly attributable to the improved displacement transfer capability of the more flexible matrices. This effect can easily be concluded from the Reuss and Voigt bounds, Eqs. (30) and (31). The Reuss bound gives a benchmark straight line versus f, independent of materials elastic moduli. As the elastic moduli of the matrix are the same as those of the magnetostrictive particles, the Voigt bound coincides with the Reuss benchmark line. But as the matrix is much softer than the magnetostrictive particles, the Voigt bound moves up toward much larger values, and approaches the values for the single-phase magnetostrictive materials $(f=1)$ as $G_1\to 0$; in reverse, the Voigt bound moves down toward much lower values as the matrix is much stiffer than the magnetostrictive particles, and approaches zero as $G_1/G_2\to\infty$. The stiff matrix suppresses the deformation of the magnetostrictive particles.

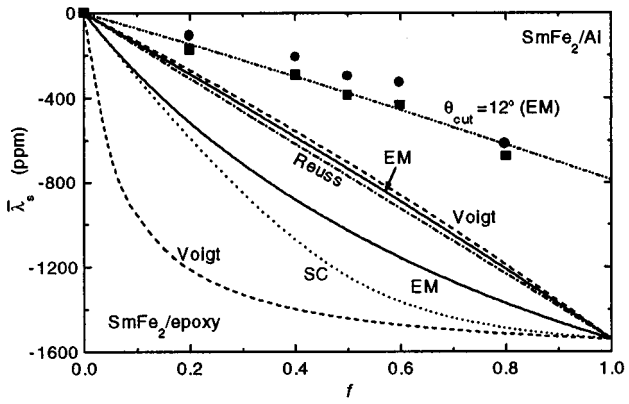

FIG. 1. The effective saturation magnetostriction of $SmFe_2$/Al (above the Reuss bound line) and $SmFe_2$/epoxy (below the Reuss bound line) isotropic composites with completely random orientation of spherical $SmFe_2$ particles. Voigt bounds for these two composites and a SC calculation for $SmFe_2$/epoxy composite are shown for comparison. The solid dots are experimental data for $SmFe_2$/Al composite (Ref. 6). For illustration and comparison, the calculated results are also shown for a uniform orientation distribution of the X_3' axis of $SmFe_2$ crystallites with respect to the sample axis X_3 within a cone angle of 12°.

As seen from the effective-medium formulation (29) and the Reuss and Voigt bounds, Eqs. (30) and (31), the effective magnetostriction of the particulate composites is strongly dependent on the orientations of the magnetostrictive particles (this is discussed further in the following section). This is also true even for the case of elastically isotropic particles. For comparison with the calculations in the case of completely randomly oriented particles, in Fig. 1 we also present the results for the $SmFe_2$/Al composite by simply considering a uniform orientation distribution of the elastically isotropic, spherical $SmFe_2$ particles between $\theta=0$ and 12° (and the Euler angles ψ and ϕ randomly varying from 0 to 2π). The recent experimental data for the $SmFe_2$/Al composite[6] is also shown for illustration.

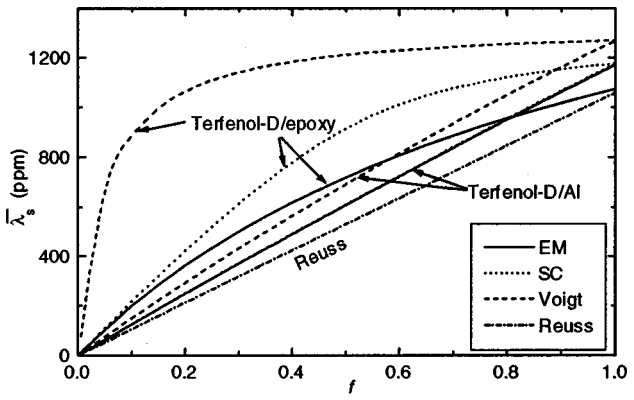

FIG. 2. The effective saturation magnetostriction of Terfenol-D/epoxy and Terfenol/Al isotropic composites with completely random orientation of spherical Terfenol-D particles. The EM and SC calculations, and Voigt and Reuss bounds for these two composites are shown for comparison. The EM and SC results for Terfenol/Al composite are nearly the same.

Similarly, for Terfenol-D/epoxy or Al composites where Terfenol-D particles are not elastically isotropic, i.e., $c_{11}-c_{12}\neq 2c_{44}$, the softer the matrix, the larger the effective magnetostriction of the composite (Fig. 2). The Voigt approximation yields upper bounds for these two Terfenol-D particulate reinforced composites and the Reuss bound is a lower one, since $G_1/c_{44}<1$. But as $f=1$, the effective-medium formulation and the Reuss and Voigt bounds give different values in the case where $c_{11}-c_{12}\neq 2c_{44}$, unlike those results shown in Fig. 1.

For illustration and comparison, Figs. 1 and 2 show predictions of two common first-order effective-medium approximations. One is a non-self-consistent effective-medium (EM) approximation, namely that in which the effective medium in which the magnetostrictive particles are embedded corresponds to the matrix phase alone. Phenomenologically, this corresponds to the Maxwell-Garnett approximation for the transport problem,[13] or the Mori-Tanaka approximation for the elastic problem.[19] In essence, it is a simple effective-medium approximation that is known to be reasonable for matrix-based composites with particulate microstructures. However, when the particles agglomerate, it is more reasonable to consider the constituent phases embedded in an effective medium that corresponds to the overall composite itself but with the moduli that must be determined self-consistently, which is the self-consistent (SC) effective-medium approximation. Phenomenologically, this SC approximation corresponds to the Bruggeman-Landauer self-consistent approximation for transport problem or the Kröner-Hill-Budiansky self-consistent approximation for the elastic problem.[20] At low volume fractions the two forms of the effective-medium solutions give only slightly different results but the difference becomes more marked with increasing volume fraction. This is especially so for the case where there is a large difference between the elastic moduli of the matrix and the magnetostrictive particles (e.g., $SmFe_2$/epoxy and Terfenol-D/epoxy composites). The SC solution predicts a consistently higher magnetostriction than the simple EM solution, since the former predicts a higher G^* than the latter. As apparently seen from the predictions

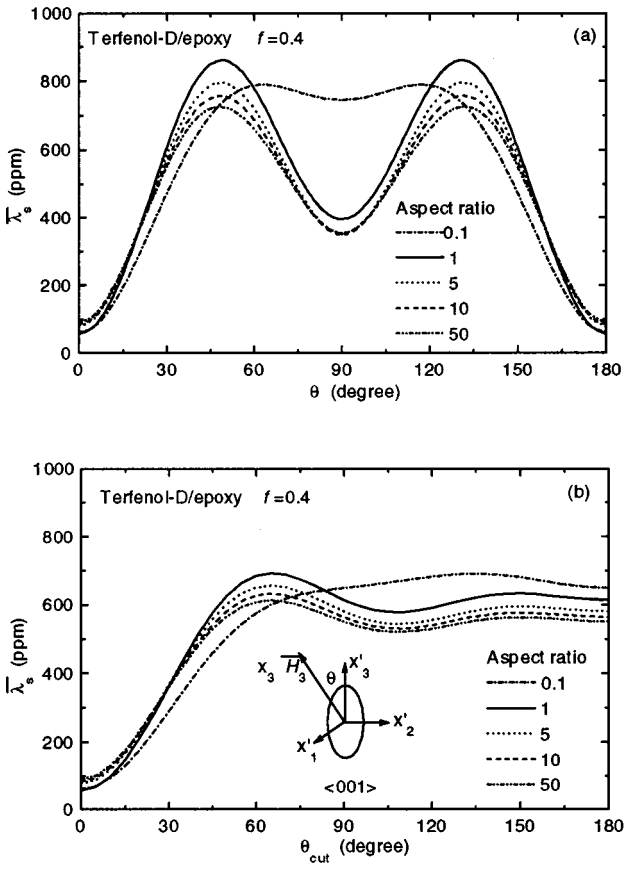

FIG. 3. The effective saturation magnetostriction (EM predictions) of 40 vol % Terfenol-D/epoxy composites for various aspect ratios with (a) an identical orientation and (b) a uniform orientation distribution of the ⟨001⟩ type ellipsoidal Terfenol-D particles (see text).

for the composites of Terfenol-D (Fig. 2), the simple EM solution does not give the same $\bar{\lambda}_s$ value for the Terfenol-D/epoxy and Terfenol/Al systems in the limit of $f=1$. This indicates that the EM solution for $\bar{\lambda}_s$ is invalid within the high concentration range (e.g., $f>0.5$) in the case that $c_{11}-c_{12}\neq 2c_{44}$ and $G_1/c_{44}\ll 1$ (or $\gg 1$).

B. Ellipsoidal particulate and 1-3 type composites

Figures 3–5 show the predictions for the Terfenol-D/epoxy composite which contains 40 vol % the Terfenol-D crystallites with different preferred growth directions. It demonstrates that the effective magnetostriction of the composite is dependent upon the particle orientation, particle shape, and growth direction. For the Terfenol-D, the highly magnetostrictive direction is along ⟨111⟩ axis. The effective magnetostriction of the composite increases with the ⟨111⟩ directions of all crystallites oriented as completely parallel to the sample axis X_3, along which the external magnetic field $\bar{H}_3$ is applied, as possible.

Figure 3(a) shows the orientation effect of the ⟨001⟩-type ellipsoidal particle (i.e., their ellipsoidal symmetric axis growth along their local crystallographic axis, X_3') where all ellipsoidal particles are considered to identically orient along one direction of a cone angle θ about the sample axis X_3

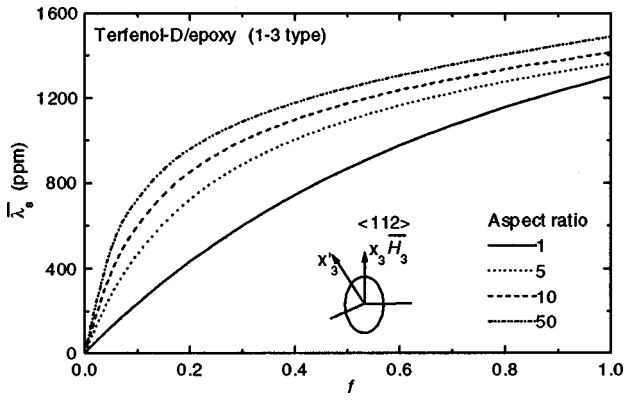

FIG. 4. The effective saturation magnetostriction (EM predictions) of 1-3 type Terfenol-D/epoxy composites for various aspect ratios with Terfenol-D crystallites grown along the $\langle 112 \rangle$ direction.

$(\overline{H}_3)$. Obviously, only when the $\langle 111 \rangle$ directions of all crystallites are identically aligned parallel to the sample X_3 axis, i.e., $\theta = 55°$, the engineering saturation magnetostriction $\overline{\lambda}_s$ reaches a maximum, and it decreases with a deviation of θ from 55°. When all ellipsoidal particles are aligned parallel to the applied magnetic field $\overline{H}_3$ (i.e., $\theta = 0$ or π), $\overline{\lambda}_s \rightarrow \sim \varepsilon_{33}^{ms} \rightarrow \sim \lambda_{100}$. As shown in Fig. 3(b), the orientation distribution of the particles also affects $\overline{\lambda}_s$. In the case of a uniform orientation distribution between $\theta = 0$ and θ_{cut} (random orientation in the X_1X_2 plane, i.e., the Euler angles ψ and ϕ randomly varying from 0 to 2π), $\overline{\lambda}_s$ reaches a maximum at about $\theta_{cut} = 65°$. The uniform distribution shifts the angle of the maximum $\overline{\lambda}_s$ from the standard 55° to 65° due to interactions between various oriented particles. Similarly, $\overline{\lambda}_s$ in this uniform distribution case increases with θ_{cut} as $\theta_{cut} < 65^o$, and decreases as $\theta_{cut} > 65°$; but $\theta_{cut} > 90°$, $\overline{\lambda}_s$ somewhat fluctuates about the effective magnetostriction for the completely random case.

In the two cases of both identical orientation and uniform orientation distribution of the $\langle 001 \rangle$-type ellipsoidal particle, the maximum $\overline{\lambda}_s$ decreases with the aspect ratio deviating from 1. In the cases of the ellipsoidal symmetric axis of all particles identically perpendicular to the sample axis X_3 [Fig. 3(a)] or random orientation [Fig. 3(b)], $\overline{\lambda}_s$ increases with the decrease in the aspect ratio, that is, oblate-shaped particles produce a larger magnetostriction than spherical, than prolate-shaped particles. Only in the case when the symmetric axes of particles almost align and are parallel to X_3, the $\overline{\lambda}_s$ will increase slightly with the aspect ratio, but still exhibits its low values $(\rightarrow \lambda_{100})$ for the crystallites with a $\langle 001 \rangle$ growth direction.

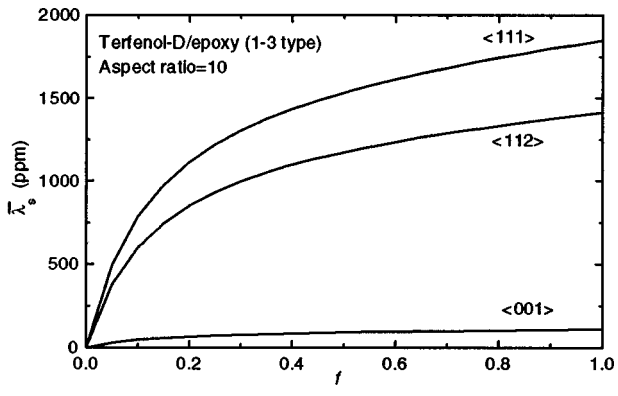

FIG. 5. The effective saturation magnetostriction (EM predictions) of 1-3 type Terfenol-D/epoxy composites for three different growth directions of Terfenol-D rods with an aspect ratio of 10.

Figure 4 shows the predictions for such a 1-3 type Terfenol-D/epoxy composite with a preferred growth direction along the $\langle 112 \rangle$ direction of Terfenol-D crystallites, which are commonly produced by the modified Bridgman and the free-standing float-zone techniques.[21] The effective magnetostriction of the 1-3 type composite increases with the aspect ratio in the whole volume fraction range. Around $f = 0.4$, the effective magnetostriction of the 1-3 type composite with the aligned rods of a large aspect ratio, can be two times larger than that of the spherical particulate composite. Similarly, when the $\langle 112 \rangle$ Terfenol-D rods do not form 1-3 connection rather than orient within a cone angle of 20° about the sample axis $X_3(\overline{H}_3)$, $\overline{\lambda}_s$ also increases to slightly little higher values, but any other orientations will result in lower $\overline{\lambda}_s$ values in comparison with the $\overline{\lambda}_s$ values of 1-3 type composites. Figure 5 shows the effect of the growth direction of the magnetostrictive crystallites in the 1-3 type Terfenol-D/epoxy composite. It is evident that the rods with their symmetric axis growing along $\langle 111 \rangle$ induce a larger effective magnetostriction than the rods with the $\langle 112 \rangle$ growth direction, and that the rods with the $\langle 001 \rangle$ growth direction do not induce significant magnetostriction of the 1-3 type composite as discussed above. Of the magnetostrictive composites, the 1-3 type composites with the rods growing along the $\langle 111 \rangle$ direction exhibit the largest saturation magnetostriction. These predictions about the effects of particle shape, orientation, and growth direction on the effective saturation magnetostriction of the composites are interesting consequences of the theory, and remain to be verified experimentally.

V. CONCLUSIONS

In this paper we have developed an effective-medium approach for the effective magnetostriction of inhomogeneous magnetostrictive materials by utilizing a Green's-function technique. In the meantime, Reuss and Voigt-type approximations are also given, which yield bounds for the effective saturation magnetostriction. For the spherical particulate and 1-3 type fibrous composites with elastically isotropic magnetostrictive crystallites, explicit approximate expressions for the effective saturation magnetostriction have been given. Numerical calculations for the effective saturation magnetostriction in $SmFe_2$/epoxy or Al and Terfenol-D/epoxy or Al composites have demonstrated that the effective saturation magnetostriction of the composites can be strongly influenced by the material constants, the volume fraction, phase connectivity, particle shape and orientation, and growth direction of the magnetostrictive crystallites. These numerical results have shown the interesting behavior of the composites; they can provide a general guideline for the evaluation

of more composite systems and thereby be used to develop criteria for choosing the best combination of different constituent materials for the magnetostrictive actuators and sensors. The present theoretical framework can also be extended, in a straightforward manner, to modeling other macroscopic properties, such as strain versus H-field behavior, hysteresis, stress and thermal effect, and ΔE effect, of the inhomogeneous magnetostrictive materials.

ACKNOWLEDGMENTS

This work was supported by the National Science Foundation, Mechanics and Materials Program, under Grant No. CMS-9625304, by the National Nature Science Foundation of China through the Outstanding Young Scientist Foundation under Grant No. 59825102, and the Ministry of Education of China.

[1] A. E. Clark, in *Ferromagnetic Materials*, edited by E. M. Wohlfarth (North-Holland, Amsterdam, 1980), Vol. 1, p. 531.
[2] B. D. Cullity, *Introduction to Magnetic Materials* (Addison-Wesley, Reading, MA, 1972), Chap. 8, p. 248.
[3] L. Sandlund, M. Fahlander, T. Cedell, A. E. Clark, J. B. Restorff, and M. Wun-Fogle, J. Appl. Phys. **75**, 5656 (1994).
[4] L. Ruiz de Angulo, J. S. Abell, and I. R. Harris, J. Magn. Magn. Mater. **157/158**, 508 (1996).
[5] F. E. Pinkerton, T. W. Capehart, J. F. Herbst, E. G. Brewer, and C. B. Murphy, Appl. Phys. Lett. **70**, 2601 (1997).
[6] J. F. Herbst, T. W. Capehart, and F. E. Pinkerton, Appl. Phys. Lett. **70**, 3041 (1997).
[7] M. Anjanappa and Y. Wu, Smart Mater. Struct. **6**, 393 (1997).
[8] F. E. Pinkerton, J. F. Herbst, T. W. Capehart, M. S. Meyer, and W. A. Fellberg, J. Appl. Phys. **85**, 1654 (1999).
[9] N. S. Akulov, Z. Phys. **66**, 533 (1930).
[10] H. E. Callen and N. Goldberg, J. Appl. Phys. **36**, 976 (1965).
[11] M. Birsan, J. Appl. Phys. **82**, 6138 (1997).
[12] C.-W. Nan, Appl. Phys. Lett. **72**, 2897 (1998).
[13] R. Zeller and P. H. Dederichs, Phys. Status Solidi B **55**, 831 (1973); J. E. Gubernatis and J. A. Krumhansl, J. Appl. Phys. **46**, 1875 (1975); for a recent review, see C.-W. Nan, Prog. Mater. Sci. **37**, 1 (1993).
[14] C.-W. Nan, Phys. Rev. B **50**, 6082 (1994).
[15] C.-W. Nan and F.-S. Jin, Phys. Rev. B **48**, 8578 (1993); C.-W. Nan, J. Appl. Phys. **76**, 1155 (1994).
[16] J. Li and G. J. Weng, Proc. R. Soc. London, Ser. A (to be published).
[17] C. Kittel, Rev. Mod. Phys. **21**, 541 (1949).
[18] R. E. Newnham, D. P. Skinner, and L. E. Cross, Mater. Res. Bull. **13**, 525 (1978).
[19] G. J. Weng, J. Mech. Phys. Solids **38**, 419 (1990).
[20] C.-W. Nan and D. R. Clarke, J. Am. Ceram. Soc. **80**, 1333 (1997).
[21] D. Jiles, *Introduction to Magnetics and Magnetic Materials* (Chapman and Hall, London, 1994), Chap. 5.